

Nature **390**, 249 (1997); J. F. Tomb *et al.*, *Nature* **388**, 539 (1997).

2. C. M. Fraser *et al.*, *Science* **270**, 397 (1995). Updated annotation of the genome is available from the TIGR Microbial Database (www.tigr.org/tdb/mdb/mdb.html).
3. R. Himmelreich *et al.*, *Nucleic Acids Res.* **24**, 4420 (1996).
4. H. J. Morowitz, *Isr. J. Med. Sci.* **20**, 750 (1984); J. Maniloff, *Proc. Natl. Acad. Sci. U.S.A.* **93**, 10004 (1996).
5. S. D. Colman, p.-C. Hu, W. Litaker, K. F. Bott, *Mol. Microbiol.* **4**, 683 (1990).
6. M. G. Goebel and T. D. Petes, *Cell* **46**, 983 (1986); M. Itaya, *FEBS Lett.* **362**, 257 (1995).
7. A. R. Mushegian and E. V. Koonin, *Proc. Natl. Acad. Sci. U.S.A.* **93**, 1026 (1996).
8. R. Himmelreich, H. Plagens, H. Hilbert, B. Reiner, R. Herrmann, *Nucleic Acids Res.* **25**, 701 (1997).
9. Transposon Tn4001, originally from *Staphylococcus aureus*, was propagated in *Escherichia coli* plasmid pISM2062 (17) and then introduced into *M. genitalium* and *M. pneumoniae* cells by electroporation (18). Approximately one in 10³ to 10⁴ *M. pneumoniae* cells and one in 10⁵ to 10⁶ *M. genitalium* cells were transformed to resistance to gentamycin (Gm). Cultures were split immediately after electroporation to generate eight separate populations for each species. Each population harbored cells representing ~200 transposition events for *M. genitalium* and >1000 events for *M. pneumoniae*. These populations were allowed to recover in SP4 medium overnight, followed by growth in the presence of Gm for 2 to 4 weeks, resulting in the expansion of cell number by a factor of >10⁹. This procedure was designed to make the subsequent cloning of transposition events from nonviable cells highly improbable. Genomic DNA was isolated from mid-log cultures; 2 µg of DNA was digested with Dra I. The genomic DNA restriction digests were diluted to 5 ng/µl and fragments were circularized using DNA ligase. Transposon junctions were amplified using inverse PCR with two primers specific for the end of the transposon Tn4001. Reaction products containing oligonucleotide-encoded Eco RI and Hind III sites were digested with these enzymes and cloned into the corresponding sites in pUC18. DNA sequencing templates were prepared from selected colonies and sequences generated as described (2). Transposon junction sequences were aligned with the appropriate genomic sequence to establish the site in the genome of transposon insertion.
10. Tn4001 is a composite transposon with IS256 sequences at both ends. IS256 produces 8- and 9-base pair duplications of the target sequence at the insertion site [K. G. Dyke, S. Aubert, N. el Solh, *Plasmid* **28**, 235 (1992); L. B. Rice, L. L. Carias, S. H. Marshall, *Antimicrob. Agents Chemother.* **39**, 1147 (1995)].
11. C. E. Romero-Arroyo *et al.*, *J. Bacteriol.* **181**, 1079 (1999).
12. Supplementary data can be found at Science Online (www.sciencemag.org/feature/data/1042937.shl).
13. The proteins involved in mycoplasma adhesion have been most extensively studied in *M. pneumoniae*. For a review see D. C. Krause, *Mol. Microbiol.* **19**, 247 (1996).
14. W. Saurin' and E. Dassa, *Mol. Microbiol.* **22**, 389 (1996).
15. E. V. Koonin and P. Bork, *Trends Biochem. Sci.* **21**, 128 (1996).
16. M. K. Cho *et al.*, *Science* **286**, 2087 (1999).
17. K. L. Knudtson and F. C. Minion, *Gene* **137**, 217 (1993).
18. S. P. Reddy, W. G. Rasmussen, J. B. Baseman, *FEMS Immunol. Med. Microbiol.* **15**, 211 (1996).
19. A. L. Delcher *et al.*, *Nucleic Acids Res.* **27**, 2369 (1999).
20. The figure shows 600 *M. genitalium* sites that were unambiguously mapped onto the *M. pneumoniae* genome. The whole-genome alignment method of Delcher *et al.* (19) mapped 317 sites, but does not map sites close to insertion/deletion and rearrangement differences between the chromosomes. An additional 201 sites were mapped by searching the *M. pneumoniae* genome for matches to short sequences (200 to 400 base pairs) containing each *M. genitalium* insertion site. An additional 83 sites that were

not mappable by the above methods (because of matches to several related *M. pneumoniae* sequences) were mapped to the corresponding position within the orthologous *M. pneumoniae* gene. The *M. pneumoniae*-specific regions are from (3), with minor modifications. Each pink highlighted region contains a block of *M. pneumoniae*-specific genes and arbitrarily includes the intergenic regions flanking it.

21. In the *M. genitalium* experiments, the growth medium

is SP-4 supplemented with either glucose or fructose as indicated. In the *M. pneumoniae* experiment, the cells were grown in Hayflick's medium supplemented with glucose or fructose. Cells were grown five passages (split 1 to 10) under the indicated condition before preparation of DNA for PCR templates. This is approximately equivalent to nine doublings.

23 June 1999; accepted 20 October 1999

Functional Human Corneal Equivalents Constructed from Cell Lines

May Griffith,^{1*} Rosemarie Osborne,² Rejean Munger,¹ Xiaojuan Xiong,¹ Charles J. Doillon,³ Noelani L. C. Laycock,¹ Malik Hakim,¹ Ying Song,¹ Mitchell A. Watsky⁴

Human corneal equivalents comprising the three main layers of the cornea (epithelium, stroma, and endothelium) were constructed. Each cellular layer was fabricated from immortalized human corneal cells that were screened for use on the basis of morphological, biochemical, and electrophysiological similarity to their natural counterparts. The resulting corneal equivalents mimicked human corneas in key physical and physiological functions, including morphology, biochemical marker expression, transparency, ion and fluid transport, and gene expression. Morphological and functional equivalents to human corneas that can be produced *in vitro* have immediate applications in toxicity and drug efficacy testing, and form the basis for future development of implantable tissues.

The cornea comprises three major cellular layers: an outermost stratified squamous epithelium, a stroma with keratocytes, and an innermost monolayer of specialized endothelial cells. The structure of the cornea allows it to serve as a barrier to the outside environment and as a major element in the optical pathway of the eye (1). The cornea is transparent, avascular, and immunologically privileged (2), making it an excellent candidate for tissue engineering for transplantation. Various researchers have attempted to fabricate artificial corneas or parts of corneas *in vitro* (3), but there have been no reports of successfully reconstructed human corneas that mimic the anatomy and physiology of the human cornea.

Our objective was to develop a morphological and functional equivalent of the human cornea. Human cell lines were developed from cells isolated from the individual cellular layers of the cornea. Most were immortalized (4) by

infection with an amphotropic recombinant retrovirus containing HPV16 genes E6 and E7 (5, 6); others were immortalized by transfection (7) with mammalian expression vectors containing genes encoding SV40 large T antigen, pSV3neo (8), and adenovirus E1A 12S (9), separately or in combination. Immortalized cells had random chromosomal breaks, structural rearrangements, and, in several lines, aneuploidy (10); similar chromosomal anomalies associated with immortalization were reported in HPV E6/E7 immortalized vascular endothelial cells (6), although random structural rearrangements and aneuploidy are also present in normal human corneal cells (11). The immortalized cells also had significant telomerase activity (12) [associated with the immortalized phenotype (6)] compared to little or no activity in nonimmortalized cells.

Before use in corneal equivalents, cell lines were screened for morphological, biochemical, and electrophysiological similarities to freshly dissociated or low-passage corneal cells obtained from postmortem human corneas. Electrophysiological screening of epithelial cells by means of amphotericin-perforated patch clamping (13) showed that immortalized cells had whole-cell currents similar to those of cultured corneal epithelial cells (Fig. 1, A to F) (14). Cells with altered phenotypes and physiology (transformed cells), however, showed anomalous currents (Fig. 1, G to I). Patch clamping was also used in screening keratocyte and

¹University of Ottawa Eye Institute and Department of Cellular and Molecular Medicine, University of Ottawa, Ottawa Hospital—General Campus, Ottawa, Ontario K1H 8L6, Canada. ²Human & Environmental Safety Division, Procter & Gamble Company, Miami Valley Laboratories, Cincinnati, OH 45253, USA. ³Biomaterials Institute of Quebec, Pavillon St. Francois d'Assise, Centre Hospitalier et Universitaire de Quebec, Quebec G1L 3L5, Canada. ⁴Department of Physiology, University of Tennessee College of Medicine, Memphis, TN 38163, USA.

*To whom correspondence should be addressed. E-mail: mgriffith@ogh.on.ca

REPORTS

Fig. 1. Representative current tracings and current-voltage (*I-V*) records from cultured human corneal epithelial cells (A to C), an immortalized cell line (D to F), and a line found to be transformed rather than immortalized (G to I). A tail current protocol (tracings not shown) was used to determine reversal potentials. Tail currents were obtained by clamping cells at 0 mV, depolarizing to 100 mV, then hyperpolarizing to voltages shown on the x axis. Currents and *I-V* relations revealed similar nonselective cation and fenamate-activated K^+ currents in both cultured and immortalized epithelial cell lines. Similar currents were observed in transformed cells, regardless of cell type. This current is likely a Cl^- or nonselective cation current, as inferred from reversal potentials of 0 mV in NaCl baths, and is identical in both NaCl (not shown) and KCl baths. Pipette solution: 145 mM potassium methanesulfonate, 2.5 mM NaCl, 2.5 mM $CaCl_2$, 5 mM HEPES, and amphotericin B (240 mg/ml, Sigma). Bath solution: 149 mM NaCl, 5 mM KCl (145 mM KCl, 2.5 mM NaCl for KCl bath), 2.5 mM $CaCl_2$, 5 mM glucose, and 5 mM HEPES. Insets (in A, D, and G) are voltage-clamp protocols.

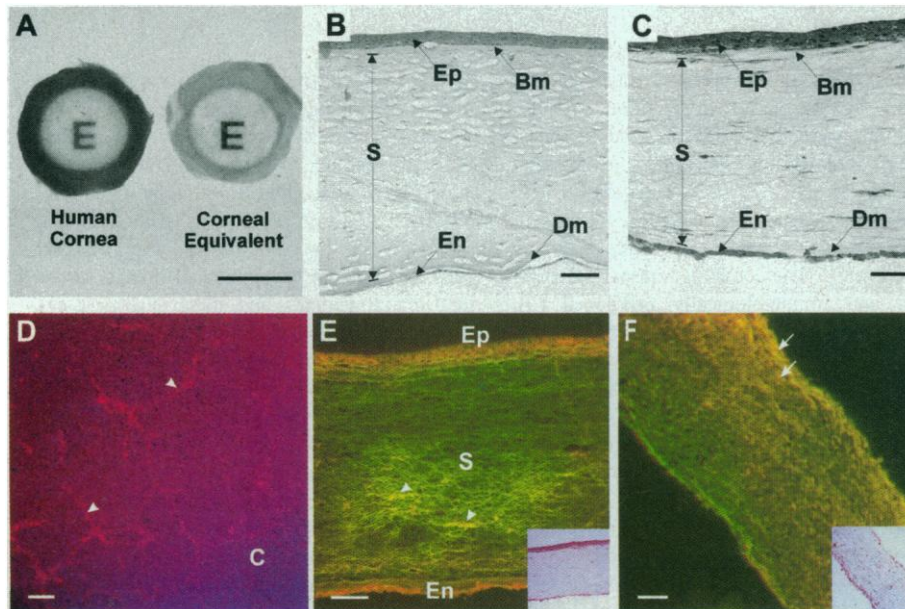
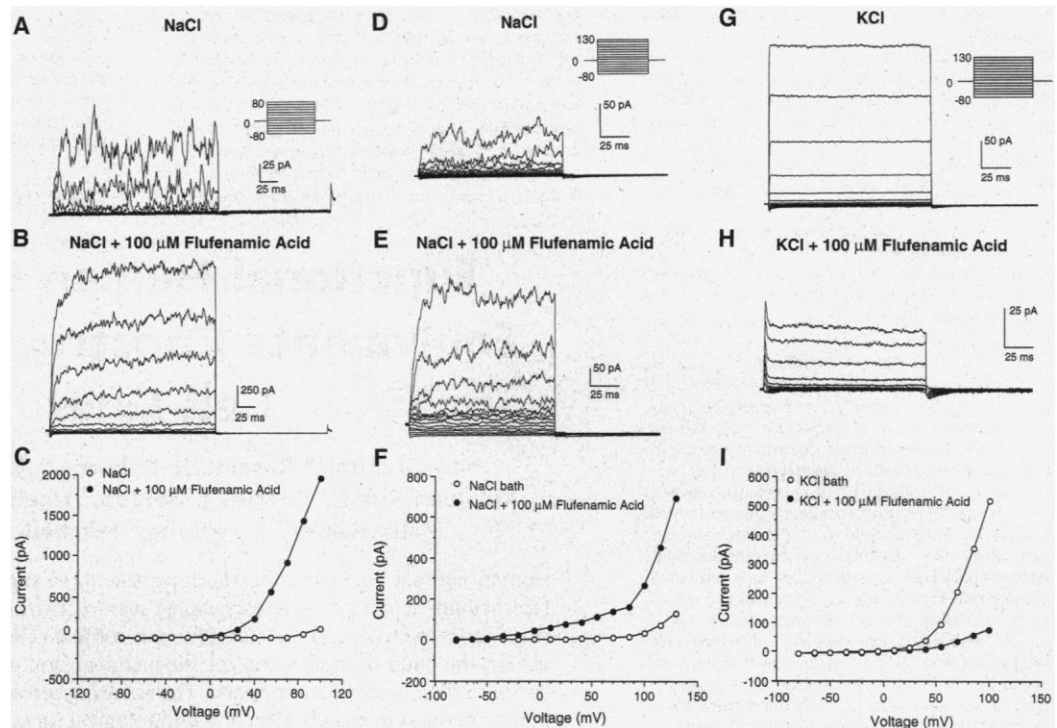


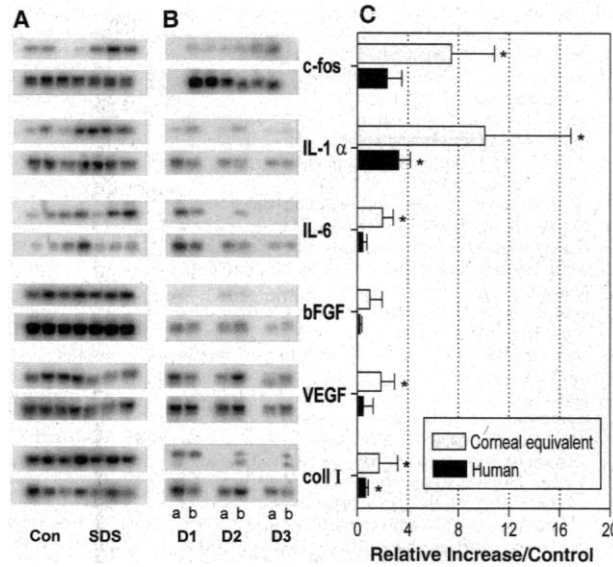
Fig. 2. (A) Postmortem human cornea with scleral rim (left) and human corneal equivalent with surrounding pseudo-sclera (right) after 2 weeks in culture. Both retained their transparency, as indicated by the clarity of the "E" beneath each cornea. Scale bar, 10 mm. (B and C) Cultured human eye bank cornea (B) and corneal equivalent (C). Both show well-defined epithelial (Ep), stromal (S), and endothelial layers (En), and acellular limiting Bowman's (Bm) and Descemet's (Dm) membranes. Interlamellar clefts in eye bank corneal stroma are storage and processing artifacts. Scale bar, 100 μm. (D) Corneal equivalent with surrounding pseudo-sclera containing microvessel-like structures (arrowheads), which bound acetylated low density lipoprotein labeled with the fluorescent probe Dil (red). The cornea (C), however, remained avascular. Scale bar, 500 μm. (E) Corneal equivalent visualized with epifluorescence by confocal microscopy. Epithelial (Ep) and endothelial (En) layers are distinct (red), and keratocytes (arrowheads) are present in the collagenous stromal matrix (S, green). Scale bar, 100 μm. (F) Cornea constructed with cell lines deemed transformed by electrophysiology. The three main layers are not readily distinguishable, and transformed epithelial cells (arrows) are seen invading the stroma. Scale bar, 100 μm. Insets (in E and F) are hematoxylin and eosin-stained sections of the same tissues.

endothelial lines. Lines with whole-cell currents closest to those of corresponding normal cells were identified; phenotypes were confirmed by expression of appropriate biochemical markers (15).

After cell lines were screened and chosen, the corneal tissue layers were constructed. Other investigators have used natural and synthetic polymers to produce scaffolds for engineered tissues (3, 16). For a tissue matrix, we used a collagen-chondroitin sulfate substrate cross-linked with 0.02 to 0.04% glutaraldehyde, then treated with glycine to remove unbound glutaraldehyde. Stromal, epithelial, and endothelial layers were created by mixing cells into, layering cells below, and layering cells on top of this substrate, respectively (17) (Fig. 2A). Constructs were typically maintained in tissue culture medium 199 with 10% fetal bovine serum, 1% insulin-transferrin-selenium, and gentamicin. We also used a serum-free medium (18) for optimal growth under defined conditions. Both media contained protease inhibitor and ascorbic acid (19) to retard cellular degradation of the matrix and to stimulate collagen synthesis. Once the epithelium at the bottom of the insert was confluent, it was exposed to air to allow differentiation into multilayers. Corneal equivalents were also successfully constructed in the reverse order (with corneal endothelium at the bottom and the air-liquid interface on top) and from low-passage primary human corneal cells, allowing for future development of transplants. Assembled corneal equivalents were allowed to

REPORTS

Fig. 3. (A) Representative Southern blots of RT-PCR products from human corneal equivalents treated with 5% SDS or medium alone (Con). 18S internal standards are shown below each set. **(B)** Southern blots of RT-PCR products from three sets of human cornea donors (D1 to D3). One cornea in each pair was a control (a); the other was treated with 5% SDS (b). 18S internal standards are shown below each set. **(C)** Changes in mRNA expression in human corneas and corneal equivalents with SDS. The intensity of mRNA bands was normalized to corresponding 18S bands. Changes in gene expression are shown as relative increase over control. Corneal equivalents, $n = 8$ for control and $n = 9$ for treated groups; human corneas, $n = 3$ for control and treated groups. * $P < 0.05$ versus control (t test).



differentiate for 2 weeks before use.

The corneal equivalents resembled human corneas in gross morphology, transparency (Fig. 2A), and histology (Fig. 2, B and C). Transmission electron microscopy showed structures of healthy, actively metabolizing cells (electron-lucent nuclei, numerous mitochondria, extensive rough endoplasmic reticulum) (20). Modifications, such as incorporation of fibrin (21), produced matrix that supported angiogenesis so the avascular cornea could be surrounded with vascularized matrix to produce a single cornea-pseudosclera construct (Fig. 2D).

The most successful multilayered corneal equivalents (Fig. 2E) were constructed from immortalized cell lines with appropriate ion channel activities (Fig. 1). Cell lines with cur-

rents indicating abnormal physiological function (Fig. 1, G to I) resulted in unsuccessful constructs (Fig. 2F). Epithelial cells showing abnormal currents stained positively for epithelial-specific keratin 12, which demonstrates the need for functional testing of cell lines in addition to immunohistochemical screening. Electrophysiological screening was therefore effective for identification of cell lines with phenotypes similar to those of low-passage or freshly dissociated human corneal cells.

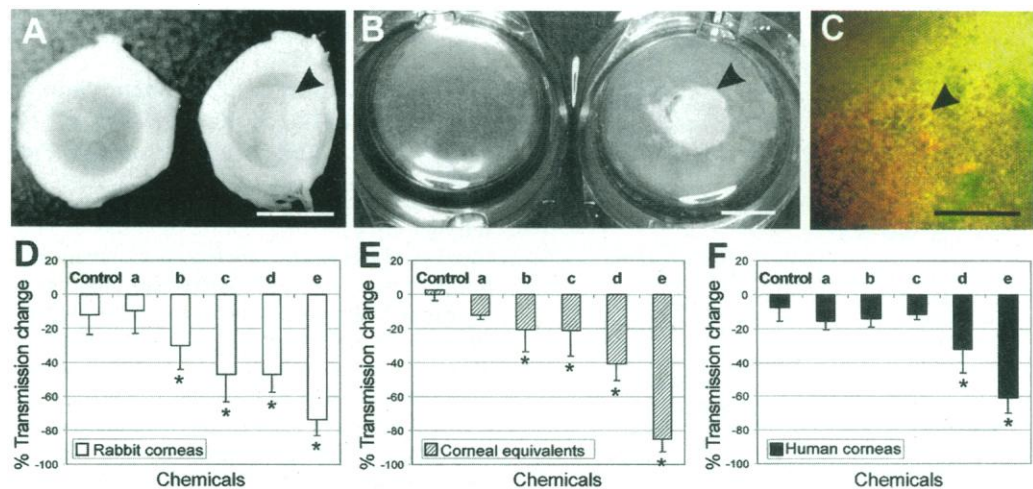
To test the physiological function of the corneal equivalents, we evaluated stromal swelling, gene expression, and tissue transparency. Optimal stromal hydration is maintained in the human cornea by the pumping action of the specialized endothelium (22). Exposure of

human corneal endothelium to ouabain (100 μ M) has been shown to disrupt pumping and increase stromal thickness [by 16% within 2 hours (23)]. Ouabain caused swelling of the corneal equivalents from 878 μ m to 1077 μ m, an increase of 22.7% ($n = 5$), as measured by optical coherence tomography (OCT) (24). Control corneal equivalents showed slight thinning by 44 μ m or 5.4% (from 813 μ m to 769 μ m; $n = 4$), likely the result of an active pump. The corneal equivalents were thus similar to human corneas in both stromal swelling and a physiologically active endothelium.

We used the reverse transcription polymerase chain reaction (RT-PCR) to examine changes in gene expression in injured corneal equivalents and human eye bank corneas (25). Corneas and corneal equivalents were exposed to 5% SDS, a surfactant that causes mild injury to the cornea (26). SDS exposure resulted in increased mRNA for genes involved in corneal wound healing [*c-fos*; the genes encoding cytokines interleukin-1 (IL-1), IL-6, basic fibroblast growth factor (bFGF), and vascular endothelial growth factor (VEGF); and the gene encoding type I collagen (Coll I)] (27) in both fabricated and eye bank corneas (Fig. 3). Fabricated corneas showed greater sensitivity, possibly because they are healthier tissues than eye bank corneas available for research.

To further evaluate the corneal equivalents, we examined changes in light transmission after exposure to chemicals, comparing responses to those of human and rabbit corneas [the standard in ocular toxicology tests (26)]. We observed opacification (Fig. 4, A and B) with increased cell death (Fig. 4C) (28) within the treatment zone of all three types of corneas. Changes in the transparency of corneal equivalents in response to chemicals (29) were similar to those observed in human and rabbit

Fig. 4. Human eye bank corneas (A) and corneal equivalents (**B**) treated on their epithelium for 5 min with 100 μ l of DMEM (control; left cornea) or 70% dimethyl dialkyl ammonium chloride (right cornea), an ocular irritant. Treated corneas show opacification of treatment areas (arrowheads). Scale bar, 10 mm. **(C)** Treated corneal equivalent stained with live/dead stain. Red (arrowhead) indicates area of dead cells; green indicates live cells. Scale bar, 10 mm. **(D to F)** Changes in light transmission through **(D)** rabbit corneas, **(E)** corneal equivalents, and **(F)** human corneas treated for 5 min with 100 μ l of DMEM (control); **(a)** artificial tears (0.3% hydroxymethylcellulose, 0.1% dextran, polyquad preservative); **(b)** anionic surfactant mixture (20% alkyl ethoxysulfate, 5% alkyl sulfate); **(c)** anionic surfactant mixture (30% alkyl benzene sulfonate, 15% alcohol ethoxylate); **(d)** cationic surfactant (50% trimethyl alkyl ammonium chloride); and **(e)** cationic surfactant (70% dimethyl dialkyl ammonium chloride). Historical rabbit low volume eye test (24) maximum average scores for



these substances were 27.2 (b), 55.7 (c), 93.0 (d), and 109.3 (e), where a higher score indicates a greater degree of corneal opacification. Human corneas, $n = 4$ for each chemical; corneal equivalents, $n = 5$ for each chemical; rabbit corneas, control group, $n = 12$; all other groups, $n = 17$. * $P < 0.05$ versus control (ANOVA).

corneas (Fig. 4, D to F). These results showed that the corneal equivalents had an active response to different grades of injury, an important functional characteristic of human corneas.

These engineered corneal equivalents have immediate applications as human ocular irritancy models for evaluating new chemicals and drugs, as alternatives to animals (30), and in drug efficacy testing such as for wound healing. The corneal equivalents can also be used in biomedical research, for example, to study wound healing and cell-matrix interactions. This technology provides a strong basis for the development of temporary or permanent cornea replacements with low rejection rates. Future research could lead to readily available, complex engineered tissues that reproduce their natural human counterparts and are suitable for implants, transplants, and biomedical research.

References and Notes

1. D. G. Pitts, in *Environmental Vision*, D. E. Pitts and R. N. Kleinstein, Eds. (Butterworth-Heinemann, Boston, 1994), chap. 6.
2. M. J. Jager et al., *Eye* **9**, 241 (1995).
3. Y. Minami, H. Sugihara, S. Oono, *Invest. Ophthalmol. Visual Sci.* **34**, 2316 (1993); J. D. Zieske et al., *Exp. Cell Res.* **214**, 621 (1994); C. R. Kahn, E. Young, I. H. Lee, J. S. Rhim, *Invest. Ophthalmol. Visual Sci.* **34**, 1983 (1993); K. Araki-Sasaki et al., *Invest. Ophthalmol. Visual Sci.* **36**, 614 (1995); L. Germain et al., *Pathobiology* **67**, 140 (1999).
4. "Immortalized cells" are cells with extended life-spans that retain characteristics of low-passage or freshly dissociated cells (contact inhibition, substrate-dependent growth, but no senescence or culture-related phenotypic changes after 8 to 10 passages).
5. C. L. Halbert, G. W. Demers, D. A. Galloway, *J. Virol.* **65**, 473 (1991); *J. Virol.* **66**, 2125 (1992). Viral producer cell line PA317LXSN 16E6E7 (American Type Culture Collection) was used.
6. J. S. Rhim et al., *Carcinogenesis* **19**, 673 (1998).
7. R. E. Kingston, in *Current Protocols Molecular Biology*, F. M. Ausubel et al., Eds. (Wiley, New York, 1997), pp. 9.0.1-9.1.11.
8. T. M. Bryan and R. R. Reddel, *Crit. Rev. Oncog.* **5**, 331 (1994); P. J. Southern and P. Berg, *J. Mol. Appl. Genet.* **1**, 327 (1982).
9. F. L. Graham and A. J. van der Eb, *Virology* **52**, 456 (1973); M. P. Quinlan, *Oncogene* **9**, 2639 (1994).
10. Cytogenetic analyses were performed by H. S. Wang (Cytogenetics Laboratory, Children's Hospital of Eastern Ontario, Ottawa) using routine G-banding techniques with 400- to 450-band resolution.
11. M. J. Pettenati et al., *Hum. Genet.* **101**, 26 (1997).
12. TeloQuant Telomeric Repeat Amplification Protocol kit (Pharmingen Canada).
13. J. L. Rae, K. E. Cooper, P. Gates, M. A. Watsky, *Br. J. Neurosci. Methods* **37**, 15 (1991).
14. C. Bockman, C. M. Griffith, M. A. Watsky, *Invest. Ophthalmol. Visual Sci.* **39**, 1143 (1998).
15. Epithelial cells showed corneal epithelial-specific keratin 12 staining [A. Schermer, S. Galvin, T. T. Sun, *J. Cell Biol.* **103**, 49 (1986)] with AE5 antibody (ICN Biochemicals, Aurora, OH). Stromal cells stained for vimentin (Roche Diagnostics, Montreal). Endothelial cells expressed $\alpha 2$ (VII) collagen mRNA [Y. Muragaki et al., *J. Biol. Chem.* **266**, 7721 (1991)] and lacked keratin 12 staining.
16. E. Bell, H. P. Ehrlich, D. J. Buttle, T. Nakatsuji, *Science* **211**, 1052 (1981); M. S. Shoichet and J. A. Hubell, Eds., *Polymers for Tissue Engineering* (VSP, Utrecht, Netherlands, 1998).
17. Cell lines producing successful constructs were from young donors, were immortalized with HPV E6/E7, and had appropriate electrophysiological responses.
18. M. Griffith et al., in preparation.
19. W. W. Y. Kao, R. A. Berg, D. J. Prockop, *Biochim.*

- Biophys. Acta* **411**, 202 (1975); C. J. Doillon, F. H. Silver, R. A. Berg, *Biomaterials* **8**, 195 (1987).
20. M. Griffith et al., unpublished data.
21. R. Janvier, A. Sourla, M. Koutsilieris, C. J. Doillon, *Anticancer Res.* **17**, 1551 (1997).
22. M. A. Watsky, T. W. Olsen, H. F. Edelhauser, in *Duane's Foundations of Clinical Ophthalmology*, B. Tasman and E. Jaeger, Eds. (Lippincott, Philadelphia, 1995), vol. 2, chap. 4.
23. D. H. Geroski, J. C. Kies, and H. F. Edelhauser [*Curr. Eye Res.* **3**, 331 (1984)] showed that 100 μ M ouabain causes swelling of human corneas (41 μ m per hour); after 2 hours corneas would swell by 82 μ m (16%).
24. Constructs, with epithelium sealed with silicone oil to prevent movement of water across the anterior surface, were measured using OCT (Zeiss-Humphrey, San Leandro, CA). The average change in thickness was calculated from four to six measurements before and after treatment of the endothelial surface for 2 hours with 100 μ M ouabain or Dulbecco's modified Eagle's medium alone (DMEM, Gibco).
25. Corneal equivalents and human eye bank corneas were treated with 5% SDS or medium 199 alone (controls) for 3 min. After a 1-hour recovery period, total RNA was extracted and mRNA was reverse-transcribed. Specific cDNA was amplified by PCR using Taq polymerase (Gibco) and primer pairs specific for human nucleotide sequences [for *c-fos*, sense (S): 5'-CTTCAACGACAGC-TACGAGG, antisense (A): 5'-CTGTCATGGTCTTCA-CAACG; for IL-1 α , S: 5'-ATCCTGAATGACGCCCTCAA, A: 5'-GGATGGGCAACTGATGTGAA; for IL-6, S: 5'-AAT-TCGGTACATCCTCGACG, A: 5'-CGGCAGAATGAGAT-GAGTTG; for bFGF (FGF-2), S: 5'-GAGAAGAGCGAC-CCTCACA, A: 5'-TAGCTTTCTGCCAGGTCC; for VEGF, S: 5'-ACTTTCTGCTGCTTGGGTG, A: 5'-TGCTGTAG-GAAGCTCATCTC; for Coll I, S: 5'-GGTGATGCTGGTC-CTGTT, A: 5'-GTCCTGGGGTCTTCTGCT]. 18S rRNA primers and Competimers (QuantumRNA 18 Internal Standards Kit; Ambion, Austin, TX) were introduced into the PCR mixture and 18S RNA was amplified together with the gene-specific cDNA and primers, within the linear amplification range, to provide internal standards for quantifying relative differences in gene expression [W. C. Gause and J. Adamovics, in *PCR Primer: A Laboratory Manual*, C. W. Dieffenbach, Ed. (Cold Spring Harbor Laboratory Press, Plainview, NY, 1995)]. PCR products were sequenced to confirm identities. To in-

- crease the sensitivity, we transferred PCR products separated by agarose gel electrophoresis to Southern (DNA) blot substrate and hybridized them with [³²P]deoxycytidine triphosphate-labeled specific probes. Quantification was performed on a Molecular Dynamics Storm Phosphorimager.
26. J. H. Draize, G. Woodard, H. O. Calvery, *J. Pharmacol. Exp. Ther.* **82**, 377 (1944); J. F. Griffith, G. A. Nixon, R. D. Bruce, P. J. Reer, E. A. Bannan, *Toxicol. Appl. Pharmacol.* **55**, 501 (1980).
27. *c-fos*: Y. Okada et al., *Graefes Arch. Clin. Exp. Ophthalmol.* **236**, 853 (1998); IL-1 and IL-6: C. Sotozono et al., *Curr. Eye Res.* **16**, 670 (1997); bFGF: V. P. T. Hoppenreijns, E. Pels, G. F. J. M. Vrensen, W. F. Treffers, *Invest. Ophthalmol. Visual Sci.* **35**, 931 (1994); VEGF: S. Amano, R. Roban, M. Kuroki, M. Tolentino, A. P. Adams, *Invest. Ophthalmol. Visual Sci.* **39**, 18 (1998); Coll I: W. J. Power, A. H. Kaufman, J. Merayo-Lloves, V. Arrunategui-Correa, C. S. Foster, *Curr. Eye Res.* **14**, 879 (1995).
28. Live/Dead Viability/Cytotoxicity kit (Molecular Probes, Eugene, OR).
29. Corneal equivalents, rabbit corneas (PelFreez, Rogers, AR), and human eye bank corneas 1 to 4 weeks post-enucleation (Eye Bank of Canada, Toronto) were treated with 100 μ l of coded test substance for 5 min, then rinsed with phosphate-buffered saline. Transmission measurements were made with a custom-built instrument [D. Priest and R. Munger, *Invest. Ophthalmol. Visual Sci.* **39**, S352 (1998)] before (T_1) and after (T_2) chemical exposure. Responses were plotted as normalized change in transmission, $CT_n = [(T_1 - T_2)/T_2] \times 100$, and compared within and across species using analysis of variance (ANOVA).
30. International Life Sciences Institute, *J. Toxicol. Cutaneous Ocul. Toxicol.* **15**, 211 (1996).
31. Supported by grants from the Natural Sciences and Engineering Research Council of Canada, Medical Research Council-Pharmaceutical Manufacturers' Association of Canada, and the P&G International Program for Animal Alternatives. We thank S. Whelan and P. Berg for Ad5 and psv3neo plasmids, C. Smith and Ottawa Hospital Research Institute colleagues, and E. Hay and A. Tashjian Jr. for helpful insights during preparation of this manuscript.

27 August 1999; accepted 4 November 1999

Mouse Models of Tumor Development in Neurofibromatosis Type 1

Karen Cichowski,^{1*} T. Shane Shih,^{1,2*} Earlene Schmitt,^{1,3}
Sabrina Santiago,¹ Karlyne Reilly,¹ Margaret E. McLaughlin,⁴
Roderick T. Bronson,⁵ Tyler Jacks^{1,6†}

Neurofibromatosis type 1 (NF1) is a prevalent familial cancer syndrome resulting from germ line mutations in the *NF1* tumor suppressor gene. Hallmark features of the disease are the development of benign peripheral nerve sheath tumors (neurofibromas), which can progress to malignancy. Unlike humans, mice that are heterozygous for a mutation in *Nf1* do not develop neurofibromas. However, as described here, chimeric mice composed in part of *Nf1*^{-/-} cells do, which demonstrates that loss of the wild-type *Nf1* allele is rate-limiting in tumor formation. In addition, mice that carry linked germ line mutations in *Nf1* and *p53* develop malignant peripheral nerve sheath tumors (MPNSTs), which supports a cooperative and causal role for *p53* mutations in MPNST development. These two mouse models provide the means to address fundamental aspects of disease development and to test therapeutic strategies.

Neurofibromatosis type I (NF1) affects about 1 in 3500 individuals worldwide (1). The hallmark clinical feature of the disease is

development of multiple benign neurofibromas, which can be debilitating, severely disfiguring, and, in some patients, progress to

LINKED CITATIONS

- Page 1 of 1 -



You have printed the following article:

Functional Human Corneal Equivalents Constructed from Cell Lines

May Griffith; Rosemarie Osborne; Rejean Munger; Xiaojuan Xiong; Charles J. Doillon; Noelani L. C. Laycock; Malik Hakim; Ying Song; Mitchell A. Watsky

Science, New Series, Vol. 286, No. 5447. (Dec. 10, 1999), pp. 2169-2172.

Stable URL:

<http://links.jstor.org/sici?sici=0036-8075%2819991210%293%3A286%3A5447%3C2169%3AFHCECF%3E2.0.CO%3B2-D>

This article references the following linked citations:

References and Notes

¹⁶ **Living Tissue Formed in vitro and Accepted as Skin-Equivalent Tissue of Full Thickness**

Eugene Bell; H. Paul Ehrlich; David J. Buttle; Takako Nakatsuji

Science, New Series, Vol. 211, No. 4486. (Mar. 6, 1981), pp. 1052-1054.

Stable URL:

<http://links.jstor.org/sici?sici=0036-8075%2819810306%293%3A211%3A4486%3C1052%3ALTFIVA%3E2.0.CO%3B2-2>